Electronic Supplementary Material (ESI) for Journal of Materials Chemistry A.
This journal is © The Royal Society of Chemistry 2021

Supporting Information

Efficient electronic coupling and heterogeneous charge transport of zero-dimensional Cs_4PbBr_6 perovskite emitters

Rugeng Liu,†[ab] Chun Hong Mak,†[ab] Xu Han,†[ab] Yunqi Tang,[ab] Guohua Jia,[c] Kuan-Chen Cheng, [def] Honglan Qi,[g] Xingli Zou,[h] Guizheng Zou,[i] Hsien-Yi Hsu*[ab]

[a] School of Energy and Environment&Department of Materials Science and Engineering, City University of Hong Kong, Kowloon Tong, Hong Kong, China.

[b] Shenzhen Research Institute of City University of Hong Kong, Shenzhen 518057, China.

[c] Curtin Institute of Functional Molecules and Interfaces School of Molecular and Life Sciences Curtin University GPO Box U1987, Perth, WA 6845, Australia.

[d] Graduate Institute of Food Science Technology, National Taiwan University, Taipei 10617, Taiwan (R.O.C.).

[e] Institute of Biotechnology, National Taiwan University, Taipei 10617, Taiwan (R.O.C.).

[f] Department of Medical Research, China Medical University Hospital China Medical University, Taichung, Taiwan (R.O.C).

[g] Key Laboratory of Analytical Chemistry for Life Science of Shaanxi Province,School of Chemistry and Chemical Engineering, Shaanxi Normal University, Xi'an, 710062, China.

[h] State Key Laboratory of Advanced Special Steel & Shanghai Key Laboratory of Advanced Ferrometallurgy & School of Materials Science and Engineering, Shanghai University, 99#Shangda Road, Shanghai 200444, China

[i] School of Chemistry and Chemical Engineering, Shandong University, Jinan 250100, China.

† contributing equally to this work

*Corresponding authors

E-mail: sam.hyhsu@cityu.edu.hk

Content

1. General methods.....3

2. Characterizations.....3

3. Eletrochemistry 4

4. ECL 4

Figure S1. Cs_4PbBr_6|GCE as working electrode in MeCN solution. 5

Figure S2. Steady-state photoluminescence (PL) of $CsPbBr_3$. 5

Figure S3. (a) Oxidation voltammogram of Cs_4PbBr_6 using a 1 mM solution of $TBAPF_6$ in MeCN at 2 V/s and 2.5 mV/s. (b) Oxidation peak current versus $\nu^{1/2}$. 5

Table S1. Kinetics of Cs_4PbBr_6 monitored at 520 nm at different temperatures. 6

Table S2. Kinetics of $CsPbBr_3$ *m*onitored at 515 nm at different temperatures. 6

Table S3. Activation energy and electronic coupling of $CsPbBr_3$ and Cs_4PbBr_6. 6

Table S4. Diffusion coefficients of typical electrochemical materials. 6

References 7

1. General methods

The precursors for the synthesis of hybrid perovskites including cesium bromide (CsBr, 99.999% metal based) and lead(II) bromide ($PbBr_2$, 99.999% metal based) were purchased from Alfa Aesar. Dimethyl sulfoxide (DMSO), tetrabutylammonium hexafluorophosphate ($TBAPF_6$), anhydrous acetonitrile (MeCN, 99.8%) and benzoyl peroxide (BPO) were purchased from Sigma-Aldrich (USA). Ferrocene (98%) was obtained from Aladdin Chemical Co., Ltd. (Shanghai, China). Analytical grade reagents were used.

The Cs_4PbBr_6 perovskites were prepared by following experiment procedure of the previous literature.[1] $PbBr_2$ (10 mmol) and CsBr (10 mmol) were dissolved in 10 mL DMSO, followed with the stirring for an hour. The solution was filtered, and the filtrate was then heated under 120°C for 3 h. Then the precipitates were collected with a Buchner funnel, washed with 1 mL DMSO for three times, and dried at 100 °C under vacuum overnight. The Cs_4PbBr_6 was stored under dark conditions. The Cs_4PbBr_6 were ultrasonically dispersed into toluene (0.03 g/mL). Then, 10 μL of the suspension was casted onto the glassy carbon electrode (GCE) to form Cs_4PbBr_6 | GCE.

2. Characterizations.

Scanning electron microscopy (SEM) images were recorded using a high-resolution scanning electron microscope (EVO MA10, Carl Zeiss, Germany). X-ray diffraction (XRD) spectra were collected at room temperature over a 2θ at certain range on PANalytical X-ray diffractometer (X'Pert3 Powder) using Cu-Kα radiation of 40 kV. The ultraviolet-visible (UV-VIS) absorption spectra were obtained by using an UV-Vis spectrophotometer (SHIMADZU, UV-2600, Kioto, Japan). The photoluminescence (PL) spectra were recorded by a spectrofluorometer (SHIMADZU, RF-5301PC, Kioto, Japan). Photoluminescence decay was conducted by transient photoluminescence (TRPL) spectrometer (PicoQuant Fluo Time 200). The data was recorded by a time-correlated single photon counting (TCSPC) system to explore the PL decay dynamics. The specification of laser was given as <200 ps pulses with a fluence of ~ 30 nJ/cm^2. The PL lifetime, τ_{PL}, was extracted by the software Fluofit (Picoquant). For the temperature-dependent TRPL, a cold circulating system (mrc scientific instrument WBL-100) was connected to the sample holder inside

the sample chamber of TRPL with slow N_2 stream introduced during the experiment in order to avoid any water vapor condensing on the surface of the material.

3. Eletrochemistry

For Cyclic voltammogram (CV) and electrochemiluminescence (ECL) experiments, the three-electrode conventional electrochemical cell consisted of a coiled Pt wire (0.5 mm in diameter) as a counter electrode, a Ag wire (0.5 mm in diameter) as the quasi-reference electrode, and a Pt disk inlaid in glass which bent at a 90° angle as the working electrode. The geometric area of the Pt disk electrode was 0.0314 cm^2. After each experiment, the potential of the Ag wire was calibrated with ferrocene as internal standard (0.342 V vs SCE).[2] The working electrode was sonicated in Milli-Q deionized water and then in acetone before the experiment. The clean-up procedures of counter and reference electrodes were processed by sonicating in acetone, water, and ethanol, finally were rinsed with D.I. water, dried in ambient condition and then transferred into a glovebox. For the measurement under ambient condition, the electrochemical and ECL cells with sample solution was protected with airtight sealed Teflon cap to avoid any O_2 contamination. To connect with the electrode inside the electrochemical cell, the stainless-steel rods as a conductor were driven through the cap. CV were obtained on a CH Instruments electrochemical workstation (CHI 760E, Austin, TX)

4. ECL

The ECL spectra were obtained on Princeton SPEC-10 Instruments using a charge-coupled device (CCD) camera (Trenton, NJ) cooled to – 100°C with an Acton SpectraPro 150 monochromator (Acton, MA) as the detector. The wavelength scale of the CCD camera and grating system were calibrated using a Hg/Ar pen-ray lamp from Oriel (Stratford, CT). ECL intensity-time curves were collected on an Autolab potentiostat (Ecochemie, Netherlands) connected to a photomultiplier tube (PMT, Hamamatsu, R4220p, Japan). The PMT was supplied with – 750 V from a Kepco (New York) high voltage power supply.

Figure S1. Cs_4PbBr_6|GCE as working electrode in MeCN solution.

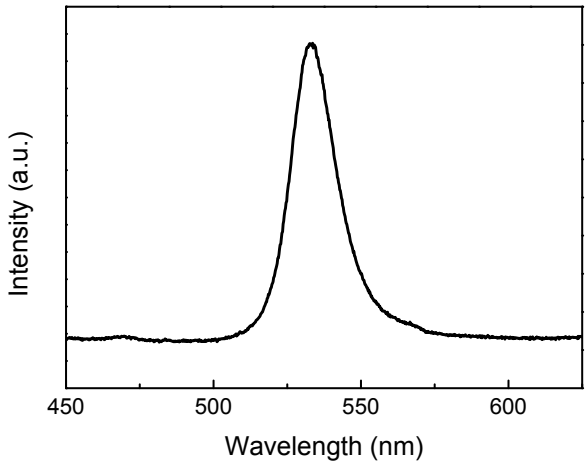

Figure S2. Steady-state photoluminescence (PL) of $CsPbBr_3$.

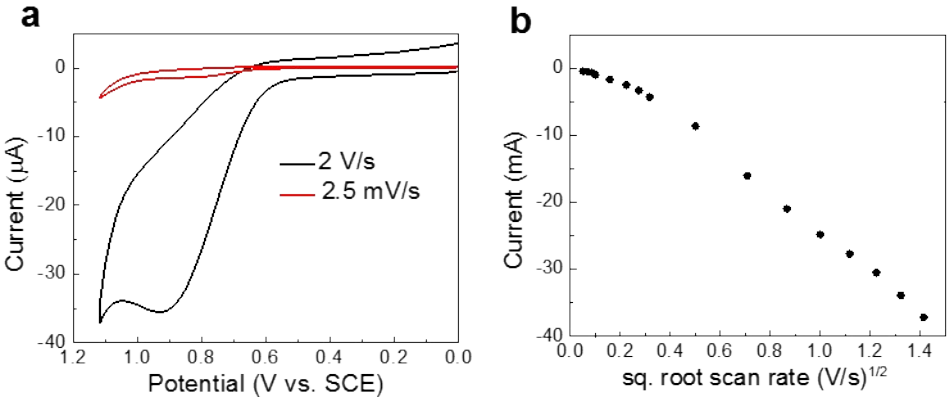

Figure S3. (a) Oxidation voltammogram of Cs_4PbBr_6 using a 1 mM solution of $TBAPF_6$ in MeCN at 2 V/s and 2.5 mV/s. (b) Oxidation peak current versus $\nu^{1/2}$.

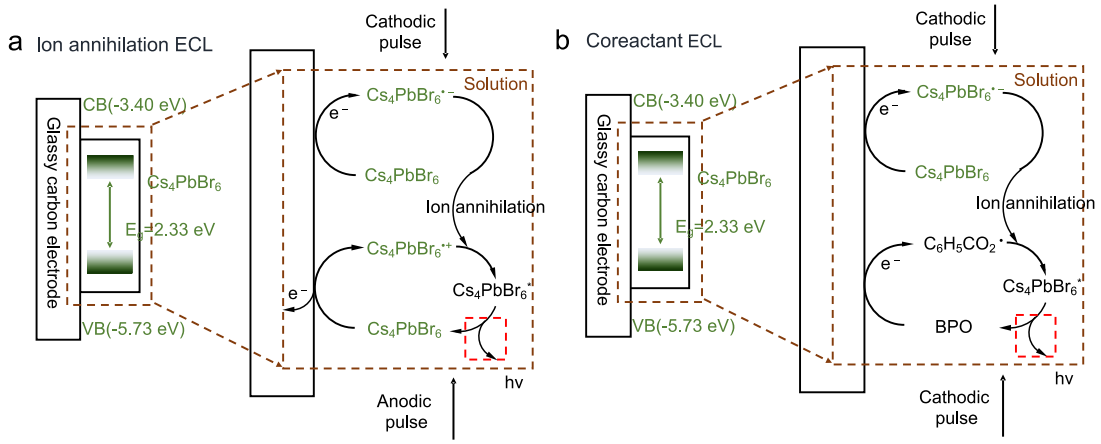

Figure S4. (a) Scheme of ion annihilation ECL process of Cs_4PbBr_6 and (b) Scheme of coreactant ECL process of Cs_4PbBr_6 when adding BPO as a coreactant.

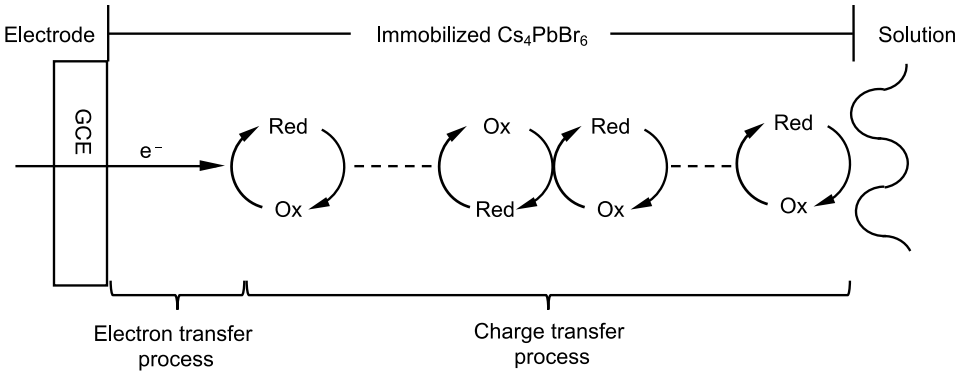

Figure S5. Schematic depiction of charge-transfer processes of immobilized Cs_4PbBr_6 on GCE. Modified from J. Phys. Chem. 1984, 88, 5274-5280.[3] Copyright 1984 American Chemical Society.

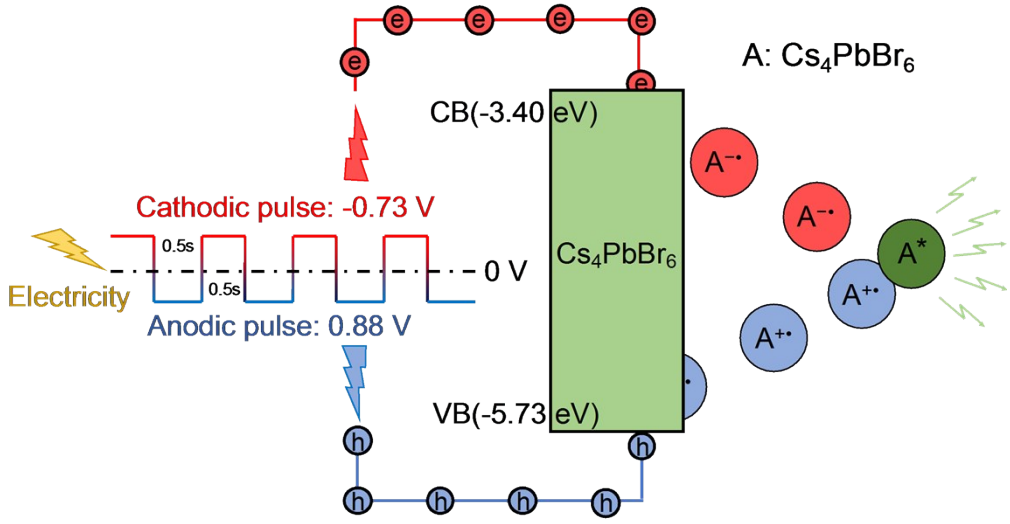

Figure S6. The generation of radical cations and anions of Cs_4PbBr_6 by applying stepped potentials.

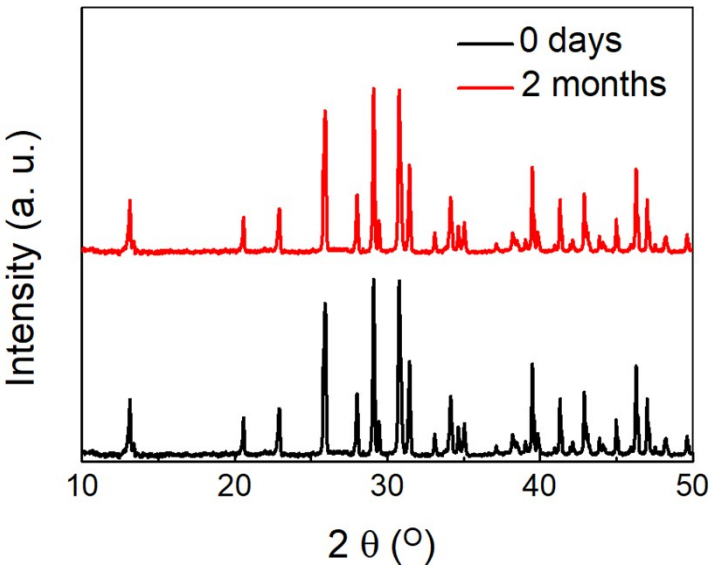

Figure S7. X-ray diffraction patterns of Cs_4PbBr_6 over a period of two months under ambient atmosphere.

Table S1. Kinetics of Cs_4PbBr_6 monitored at 520 nm at different temperatures.

Temperature (°C)	τ_1/ns (α_1)	τ_2/ns (α_2)	$<\tau>$[a]/ns	χ^2
35	3.710(79.94)	21.96(20.06)	7.37	0.834
25	4.354(83.61)	30.06(16.39)	8.57	0.824
15	5.037(84.59)	33.04(15.41)	9.35	0.996
5	6.102(83.64)	33.07(16.36)	10.51	0.900
-5	6.443(85.73)	39.43(14.27)	11.15	0.905
-15	7.532(86.06)	43.78(13.94)	12.59	0.918
-25	8.836(86.35)	49.45(13.62)	14.38	0.948

[a] $\langle\tau\rangle=\sum_i \alpha_i \tau_i$

Table S2. Kinetics of $CsPbBr_3$ ***m***onitored at 515 nm at different temperatures.

Temperature (°C)	τ_1/ns (α_1)	τ_2/ns (α_2)	$<\tau>$[a]/ns	χ^2
35	6.033(83.76)	37.75(16.24)	11.19	0.811
25	6.313(83.28)	39.21(16.72)	11.81	0.823
15	6.916(83.32)	40.02(16.68)	12.44	0.800
5	7.179(83.63)	41.56(16.37)	12.81	0.806
-5	7.217(82.45)	42.12(17.55)	13.34	0.806
-15	7.706(81.72)	42.32(18.28)	14.03	0.813
-25	8.244(82.36)	43.31(17.64)	14.43	0.817

[a] $\langle\tau\rangle=\sum_i \alpha_i \tau_i$

Table S3. Activation energy and electronic coupling of $CsPbBr_3$ and Cs_4PbBr_6.

Sample		Activation Energy (Ea) / meV	electronic coupling ($\lvert H_{AB}\rvert$) / cm^{-1}
$CsPbBr_3$	$<\tau>$	116	0.085
	τ_1	108	0.079
	τ_2	231	0.516
Cs_4PbBr_6	$<\tau>$	106	0.309
	τ_1	103	0.129
	τ_2	202	0.762

Table S4. Diffusion coefficients of typically immobilized redox (electroactive) species.

Material	Material status	Scan range	Diffusion coefficient / $cm^2\ s^{-1}$	ref
Cs_4PbBr_6	Solid	1.2 ~ 0 V vs SCE	6.1×10^{-6} (reduction)	This work
			2.6×10^{-6} (oxidation)	This work
$Ru(bpy)_3^{2+}$-Nafion	Solid	0.15 ~0.85 V vs MSE	5.2×10^{-10}	4
Silica gel containing PTA	Solid	0 ~ -0.6 V vs. Ag/AgCl	1.3×10^{-6}	5
$Ru(bpy)_3^{2+}$-PSS-silica-Triton X-100	Solid	0.6 ~ 1.3 V vs Ag/AgCl	5.9×10^{-9}	6
$Ru(bpy)_3^{2+}$-Nafion/Fe_3O_4 magnetic nanoparticles	Solid	0.68~ 1.3 V vs Ag/AgCl	3.7×10^{-8}	7
$Ru(bpy)_3^{2+}$ - PSS-ORMOSILs film	Solid	0.6 ~ 1.2V vs Ag/AgCl	7.6×10^{-10}	8
$Ru(bpy)_3^{2+}$-V_2O_5/Nafion	Solid	0.85~ 1.3 V vs Ag/AgCl	1.9×10^{-9}	9
$Ru(bpy)_3^{2+}$-SWCNT-titania-Nafion	Solid	0.8 ~ 1.35 V vs Ag/AgCl	1.2×10^{-9}	10
$Ru(bpy)_3^{2+}$-MWCNT-titania-Nafion	Solid	0.8 ~ 1.35 V vs Ag/AgCl	7.9×10^{-10}	10
$Ru(bpy)_3^{2+}$ - NENTs-PSS-ORMOSILs film	Solid	0.7 ~ 1.3 V vs SCE	2.7×10^{-9}	11
$Ru(bpy)_3^{2+}$-MWCNT-ZnO-	Solid	0.75 ~ 1.35 V vs	1.37×10^{-8}	12

Nafion $H_5BW_{12}O_{40}$ xH_2O	Solid	Ag/AgCl 0 ~ -0.75 V vs. Ag/Ag_2O	4.9×10^{-7}	13

References

1. Saidaminov, M. I.; Almutlaq, J.; Sarmah, S.; Dursun, I.; Zhumekenov, A. A.; Begum, R.; Pan, J.; Cho, N.; Mohammed, O. F.; Bakr, O. M., Pure Cs4PbBr6: highly luminescent zero-dimensional perovskite solids. *ACS Energy Letters* **2016,** *1* (4), 840-845.
2. Shen, M.; Rodríguez-López, J. n.; Huang, J.; Liu, Q.; Zhu, X.-H.; Bard, A. J., Electrochemistry and Electrogenerated Chemiluminescence of Dithienylbenzothiadiazole Derivative. Differential Reactivity of Donor and Acceptor Groups and Simulations of Radical Cation− Anion and Dication− Radical Anion Annihilations. *Journal of the American Chemical Society* **2010,** *132* (38), 13453-13461.
3. Oyama, N.; Ohsaka, T.; Ushirogouchi, T., Charge-transfer reaction of metal complexes at electrode/film interfaces and in films. *The Journal of Physical Chemistry* **1984,** *88* (22), 5274-5280.
4. Martin, C. R.; Rubinstein, I.; Bard, A. J., Polymer films on electrodes. 9. Electron and mass transfer in Nafion films containing tris (2, 2'-bipyridine) ruthenium (2+). *Journal of the American Chemical Society* **1982,** *104* (18), 4817-4824.
5. Holmstrom, S. D.; Karwowska, B.; Cox, J. A.; Kulesza, P. J., Voltammetry of phosphotungstic acid immobilized in templated silica gel. *Journal of Electroanalytical Chemistry* **1998,** *456* (1-2), 239-243.
6. Wang, H.; Xu, G.; Dong, S., Electrochemiluminescence of tris (2, 2′-bipyridine) ruthenium (ii) immobilized in poly (p-styrenesulfonate)–silica–Triton X-100 composite thin-films. *Analyst* **2001,** *126* (7), 1095-1099.
7. Kim, D.-J.; Lyu, Y.-K.; Choi, H. N.; Min, I.-H.; Lee, W.-Y., Nafion-stabilized magnetic nanoparticles (Fe 3 O 4) for [Ru (bpy) 3] 2+(bpy= bipyridine) electrogenerated chemiluminescence sensor. *Chemical Communications* **2005,** (23), 2966-2968.
8. Yi, C.; Tao, Y.; Wang, B.; Chen, X., Electrochemiluminescent determination of methamphetamine based on tris (2, 2′-bipyridine) ruthenium (II) ion-association in organically modified silicate films. *Analytica chimica acta* **2005,** *541* (1-2), 73-81.
9. Choi, H. N.; Lyu, Y. K.; Lee, W. Y., Tris (2, 2′-bipyridyl) ruthenium (II) Electrogenerated Chemiluminescence Sensor Based on Sol–Gel-Derived V2O5/Nafion Composite Films. *Electroanalysis: An International Journal Devoted to Fundamental and Practical Aspects of Electroanalysis* **2006,** *18* (3), 275-281.
10. Choi, H. N.; Lee, J.-Y.; Lyu, Y.-K.; Lee, W.-Y., Tris (2, 2′-bipyridyl) ruthenium (II) electrogenerated chemiluminescence sensor based on carbon nantube dispersed in sol–gel-derived titania–Nafion composite films. *Analytica chimica acta* **2006,** *565* (1), 48-55.
11. Tao, Y.; Lin, Z.-J.; Chen, X.-M.; Chen, X.; Wang, X.-R., Tris (2, 2′-bipyridyl) ruthenium (II) electrochemiluminescence sensor based on carbon nanotube/organically modified silicate films. *Analytica chimica acta* **2007,** *594* (2), 169-174.
12. Choi, E.-J.; Kang, C.-H.; Choi, H.-N.; Lee, W.-Y., Electrogenerated Chemiluminescence Sensor Based on Tris (2, 2'-bipyridyl) ruthenium (II) Immobilized in the Composite Film of Multi-walled Carbon Nanotube/Sol-gel Zinc oxide/Nafion. *Bulletin of the Korean Chemical Society* **2009,** *30* (10), 2387-2392.
13. Adamczyk, L.; Miecznikowski, K., Solid-state electrochemical behavior of Keggin-type borotungstic acid single crystal. *Journal of Solid State Electrochemistry* **2013,** *17* (4), 1167-1173.